nature chemistry

ARTICLES

PUBLISHED ONLINE: 9 MARCH 2014 | DOI: 10.1038/NCHEM.1888

Efficient room-temperature synthesis of a highly strained carbon nanohoop fragment of buckminsterfullerene

Paul J. Evans†, Evan R. Darzi† and Ramesh Jasti*

Warped carbon-rich molecules have captured the imagination of scientists across many disciplines. Owing to their promising materials properties and challenging synthesis, strained hydrocarbons are attractive targets that push the limits of synthetic methods and molecular design. Herein we report the synthesis and characterization of [5]cycloparaphenylene ([5]CPP), a carbon nanohoop that can be envisaged as an open tubular fragment of C_{60}, the equator of C_{70} fullerene and the unit cycle of a [5,5] armchair carbon nanotube. Given its calculated 119 kcal mol^{-1} strain energy and severely distorted benzene rings, this synthesis, which employs a room-temperature macrocyclization of a diboronate precursor, single-electron reduction and elimination, is remarkably mild and high yielding (27% over three steps). Single-crystal X-ray diffraction data were obtained to confirm its geometry and previously disputed benzenoid character. First and second pseudoreversible oxidation and reduction events were observed via cyclic voltammetry. The ease of synthesis, high solubility and narrowest optical HOMO/LUMO gap of any *para*-polyphenylene synthesized make [5]CPP a desirable new material for organic electronics.

Highly strained hydrocarbons have captivated synthetic and physical organic chemists for decades because of their challenging structures and unique properties. These alarming and contorted structures have bond geometries that depart from the ideal and aromatic rings that twist out of the π plane. Just as complex natural products inform the field of the limits of synthetic technologies, imaginative geometries such as cubane or paracyclophanes act as tools to push what is believed to be synthetically achievable. In many cases these limits are surpassed and synthetic breakthroughs are made in the pursuit of new high-energy geometries. Once synthesized, these new hydrocarbons are often found to have useful properties distinct from those of their unstrained analogues. The high energy present in distressed, kinetically metastable carbon frameworks requires ingenuity to overcome, which frequently relies on high temperatures (cubane[1], corannulene[2]), photochemistry (quadricyclane[3], picotube[4]) or flash vacuum pyrolysis ([6]paracyclophane[5], C_{60} fullerene[6]).

Of particular interest is the extreme bending of aromatic systems and reaching the geometric limit of aromaticity[7,8]. Recently, cycloparaphenylenes (CPPs), hydrocarbon macrocycles that consist of distorted benzene rings linked at the *para* positions, once only the stuff of theory[9], have entered the realm of synthetic accessibility[10–13]. The field of carbon nanohoops, so-called because they are the smallest unit-cycles of armchair carbon nanotubes, has expanded rapidly because of their porous character[14], electronics[15,16], host–guest capabilities[17,18], synthetic challenge[19] and usefulness as carbon-nanotube precursors[20]. First synthesized in 2008, carbon nanohoops have now been accessed in a variety of sizes ($n = 6$–16, 18)[10–12,14,18,21–29] and with several functionalities incorporated[30–33]. The strain inherent in these distressed hydrocarbons makes synthesis, especially of the smaller [*n*]CPPs, very challenging. In addition to synthetic conquest, smaller and smaller CPPs are desired for their solubility and unique electronics. We observe a dramatic increase in strain, reduction of ring-to-ring dihedral angles and narrowing of the highest occupied molecular orbital/lowest unoccupied molecular orbital (HOMO/LUMO) gap in CPPs smaller than **[10]CPP** (Fig. 1), in contrast to the widening gap in oligoparaphenylenes[22,34].

Having successfully synthesized **[7]CPP**, an orange-emitting fluorophore, and **[6]CPP**, which packs into tubes in the solid state, we set our sights on [5]CPP. This synthetic target has

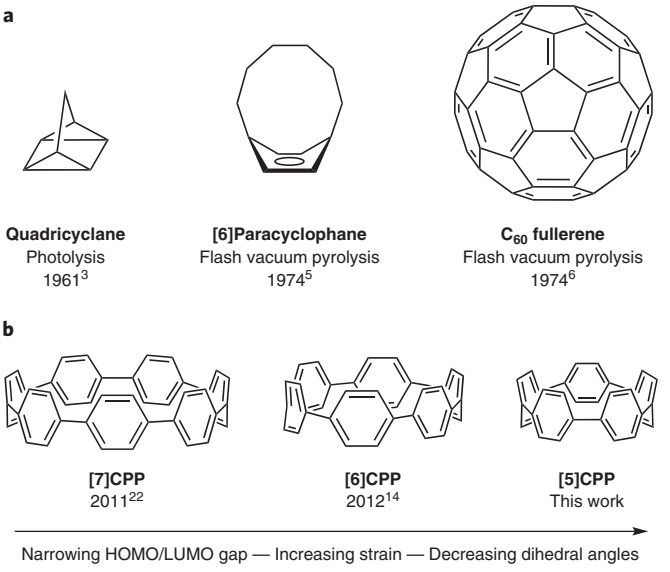

Figure 1 | Prototypical distressed hydrocarbons that have succumbed to rational organic synthesis. a, Classic examples of strained hydrocarbons that highlight the key techniques used to overcome the kinetic barrier during synthesis. **b**, The recently conquered small CPPs and trends in physical properties thereof.

Department of Chemistry and Division of Materials Science and Engineering, Boston University, Boston, Massachusetts 02215, USA.
†These authors contributed equally. *e-mail: jasti@bu.edu

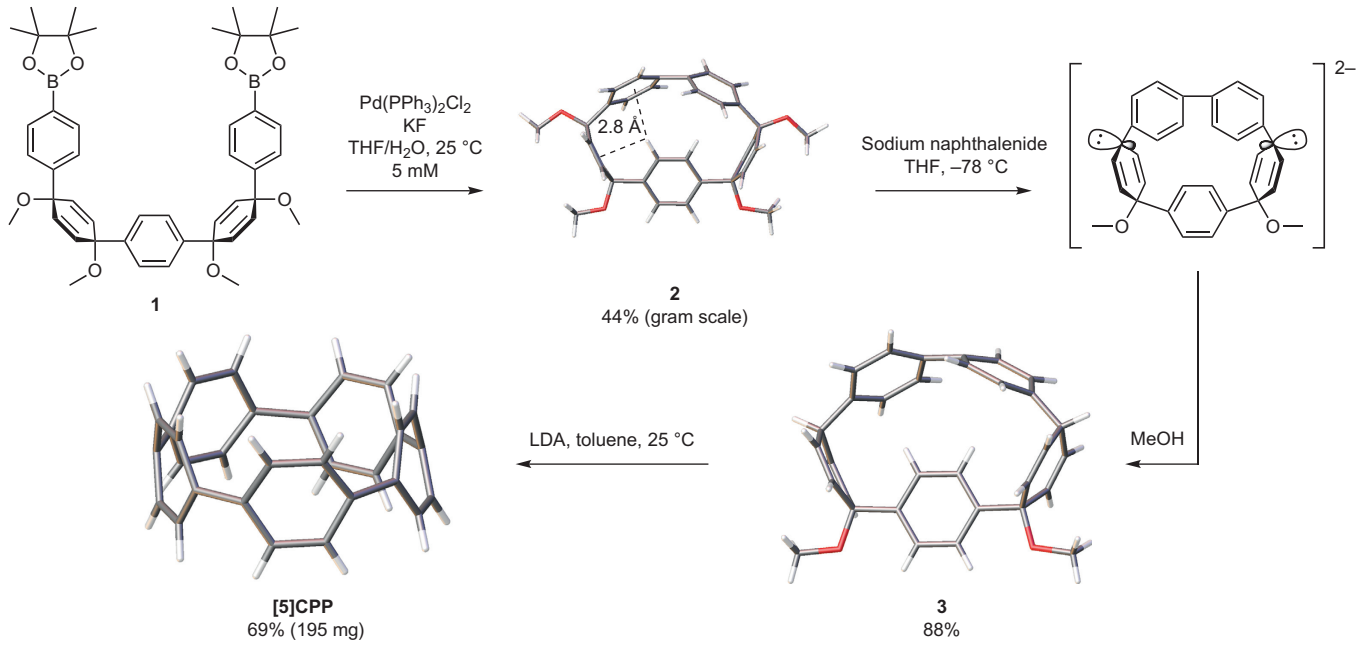

Figure 2 | A rapid synthetic route to [5]CPP. Our synthesis proceeds from the previously reported diboronate **1**, which is macrocyclized to give **2** (shown here as a DFT structure with relevant π interactions highlighted) via an intramolecular boronate homocoupling open to air. On treatment with sodium naphthalenide, **2** forms a dianion that does not convert into **[5]CPP** at −78 °C, but can be protonated by adding methanol to yield the reduced macrocycle **3** (shown as a refined crystal structure that confirms the regioselectivity of reduction). Reaction with LDA at room temperature effects a twofold E1cB elimination to give 195 mg (69%) **[5]CPP**, shown as a refined crystal structure.

119 kcal mol^{-1} strain energy, over 20 kcal mol^{-1} higher than that of **[6]CPP** (97 kcal mol^{-1}; all density functional theory (DFT) calculations were performed with GAUSSIAN09 at the B3LYP 6-31G* level of theory; all strain energies were calculated using homodesmotic reactions (see the Supplementary Information for details))[14,23,35]. **[5]CPP** also represents an open tubular fragment of buckminsterfullerene; similar fragments have heretofore been synthesized using 'top-down' methods by chemically modifying fullerenes to create substituted belts, but, to our knowledge, none have been synthesized from the bottom up without substitution[36].

In repeating our synthesis of **[10]CPP** using bisboronate **1** (Fig. 2), available on the multigram scale[18], we consistently observed the formation of small amounts of a curious new compound in our macrocyclization reactions. This material appeared to have similar NMR resonances to those of the 1,4-dimethoxycyclohexa-2,5-diene-containing macrocyclic precursors to CPPs, but with an anomalous singlet in the ^{1}H NMR spectrum at $\delta = 6.00$ ppm, further upfield than the most-shielded phenyl protons in the **[6]CPP** macrocycle ($\delta = 6.78$ ppm). Mass spectrometric and unrefined single-crystal X-ray diffraction data of this mysterious by-product confirmed, to our surprise and delight, that it was not a larger macrocycle or linear oligomer, but **2**, the result of intramolecular boronate homocoupling. These structural data allowed us to assign the singlet at $\delta =$ 6.00 ppm as the four phenyl protons on the ring between two cyclohexadiene moieties. As indicated by its multiplicity, this ring spins through the centre of the macrocycle, bringing the protons within approximately 2.8 Å of the adjacent alkenes and the centre of the nearest biphenyl ring (based on our computational investigations). The shielding cones cast by these π systems account for the dramatic upfield shift of this phenyl signal[37]. The formation of **2** is encouraged by the rigid, curved geometry of **1** in solution. With restricted rotation that allows the boron atoms to swing into proximity, intramolecular macrocyclization at high dilution becomes competitive with intermolecular processes. With this observation in mind, optimal conditions for the synthesis of **2** were developed. Using a palladium-catalysed boronate homocoupling performed under air at room temperature[38,39], macrocycle **2**, with strain energy 32 kcal mol^{-1}, was prepared easily. This discovery allowed for the synthesis of **2** on the gram scale at room temperature in one flask and facilitated a quick determination of a synthetic route to **[5]CPP** (*vide infra*).

Reduction of **2** with 5 equiv. sodium naphthalenide at −78 °C in THF surprisingly did not offer the parent CPP, as is observed with **[6]CPP**–**[12]CPP** and **[18]CPP**[12,14,18,21]. Instead, the reduction stalls at a stable dianion, which is a deep royal blue in solution. We presume that there is insufficient available energy at low temperatures to build in the 87 kcal mol^{-1} of additional strain necessary for the conversion of **2** into **[5]CPP** via elimination. Previously, the most strain overcome by these conditions was 60 kcal mol^{-1} for **[6]CPP** and 67 kcal mol^{-1} for **[7]CPP**[14,23]. Allowing this reduction to warm past −70 °C results in a colour change to dark brown and precipitation of insoluble material, which indicates rapid decomposition. Based on solubility and matrix-assisted laser desorption/ionization (MALDI) mass spectrometry data, the decomposed mixture appears qualitatively to contain oligophenylenes. Sodium naphthalenide reduction at a range of temperatures from −78 °C to room temperature does not yield more than trace (less than 1%) amounts of the desired CPP. However, quenching the dianion with methanol at −78 °C and subsequent removal of naphthalene afforded the reduced macrocycle **3** in 88% yield on the half-gram scale. The regioselectivity of this reduction was confirmed by X-ray crystallography and no regioisomers were observed in the reaction mixture.

Because **3** has the same oxidation state as **[5]CPP**, we were able to probe the E1cB elimination of two equivalents of methanol to generate **[5]CPP** at higher temperatures using a non-nucleophilic, non-reducing base to avoid the decomposition seen with the sodium naphthalenide treatment of **2**. Subjecting **3** to 30 equiv. lithium diisopropylamide (LDA) in toluene at room temperature gratifyingly afforded 195 mg of **[5]CPP**, at 69% isolated yield, as a dark-red solid with a deep ruby colour in solution.

The structure of **[5]CPP** was confirmed by NMR and infrared spectroscopy and MALDI-TOF (time of flight) mass spectroscopy.

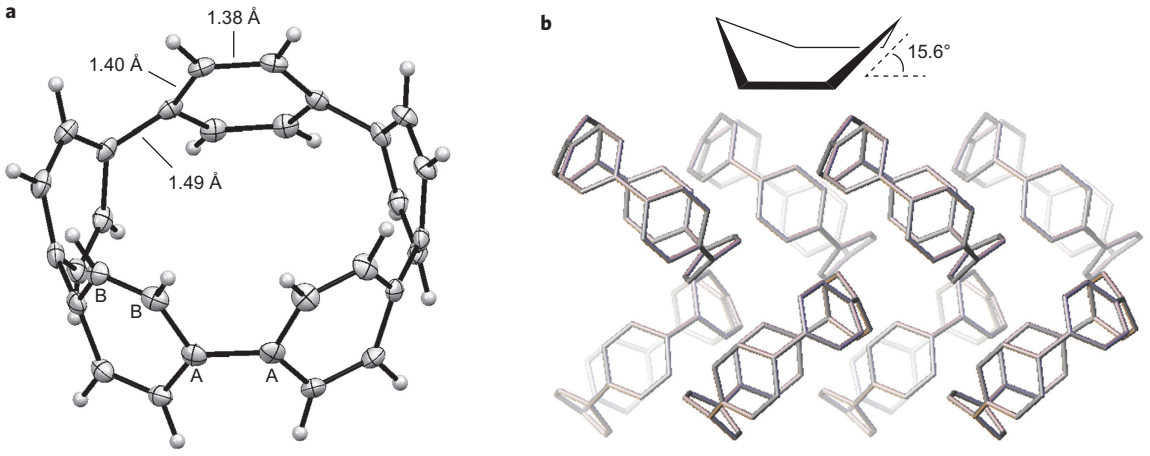

Figure 3 | Analysis of [5]CPP by X-ray diffraction crystallography. a, Solid-state bond lengths (ORTEP ellipsoids displayed at 50% probability) confirm the benzenoid nature of the phenyl rings in **[5]CPP**, despite the extreme bending out of plane (**b**). **b**, **[5]CPP** packs in a herringbone fashion, unlike **[6]CPP** but similar to all other CPPs for which crystal data have been obtained.

Interestingly, **[5]CPP** is soluble in a wide range of common organic solvents, including hydrocarbons, and aromatic, polar aprotic, halogenated and ethereal solvents. **[5]CPP**, unless stored under an inert atmosphere, decomposes into an insoluble, bright-yellow material after about 24 hours. It is possible that this is an oxidation or a nucleophilic decomposition, as is seen for [6]paracyclophane[40].

With **[5]CPP** in hand, the structure of this carbon nanohoop was investigated. The ^{1}H NMR spectrum consists of one singlet at $\delta =$ 7.86 ppm, and the ^{13}C NMR spectrum shows two signals at $\delta =$ 126.74 and 132.07 ppm. The observed isotropy suggests that at room temperature conformational changes, such as phenyl ring rotation or oscillation, make rotational isomers unobservable on the NMR timescale. The downfield shift of the proton signal in **[5]CPP** may be explained by the small phenyl–phenyl dihedral angles, calculated to average 16.4°. The tendency of these rings to remain relatively in-plane with each other encourages conjugation throughout the whole molecule and induces a deshielding ring current from the extended π system in addition to the ring currents around each phenyl ring. Wong's nucleus-independent chemical shift (NICS) calculations, which suggest that the aromaticity of individual benzene rings decreases with decreasing size in CPPs smaller than **[8]CPP**, may be taken as supporting evidence for the delocalization of the π system throughout the molecule[34]. We first observed this phenomenon in the downfield shift of the ^{1}H NMR signal for **[6]CPP** ($\delta = 7.64$) relative to that of other CPPs. Simple bending of a benzene ring alone does not account for such a dramatic downfield shift[41].

The refined crystal structure of **[5]CPP** was obtained from single crystals of **[5]CPP** that were grown from the slow evaporation of a dichloromethane and hexane solution at 0 °C in the dark (Fig. 3). Although different levels of theory have estimated **[5]CPP** to be quinoidal or benzenoid[34,42], we now confirm its benzenoid structure because the elongated phenyl–phenyl bond lengths (1.49 Å, A–A bond, Fig. 3) and the shorter and nearly equivalent phenyl bonds (1.40 Å for the A–B bond and 1.38 Å for the B–B bond, Fig. 3). The average phenyl–phenyl dihedral angle for **[5]CPP** is 12.4°, lower than the calculated 16.4° and much smaller than that of **[6]CPP**, with an average solid-state dihedral angle of 26.4°. The most striking feature of this new structure is that the nonplanar phenyl rings adopt a shallow boat conformation in the presence of considerable ring strain. The tertiary carbons in each ring are displaced out of the benzene plane by an average of 15.6°. This severe distortion is, to our knowledge, the largest of any distressed benzene isolated, with the exception of [6]- and [7]paracyclophanes[41,43,44]. This includes bent benzenes found in nature and conquered by chemists, such as those in haouamine A (13.6°)[45] and cavicularin (7.9°)[46], and the previously most-distorted CPP, **[6]CPP** (12.7°). This open-ended structure is also splayed into steeper boats than the corresponding **[5]CPP** C_{30} fragment at the equator of C_{70} fullerene (10.7°)[47] and almost as deformed as the C_{30} fragment at the rim of Scott's [5,5] carbon nanotube endcap (16.0°)[48]. The interior of **[5]CPP** has an average diameter of 6.69 Å, measured by doubling the average distance from the centroid of each ring to the centroid of the molecule. With a size comparable to that of endohedral fullerenes, it is possible that very small charged guests, such as metal ions or simple organic cations, may become encapsulated in **[5]CPP**'s inward-facing π system. Intriguingly, **[5]CPP** packs in a herringbone fashion, unlike the tubular packing observed for **[6]CPP**. The unit cells of several visually distinct crystal morphologies were analysed to confirm that this result is not anomalous.

[5]CPP absorbs very strongly in the ultraviolet region with an extinction coefficient of 5.7×10^{4} M^{-1} cm^{-1} at the maximum, 335 nm (Fig. 4). This same absorbance is observed in all CPPs and corresponds to a combination of HOMO − 2 and HOMO − 1 → LUMO and HOMO → LUMO + 1 and LUMO + 2 transitions[14,22]. Additionally, apparent by its deep-red colour, **[5]CPP** displays a very broad second absorbance band centred around 502 nm with a maximum extinction coefficient of 4.5×10^{2} M^{-1} cm^{-1}. This arises

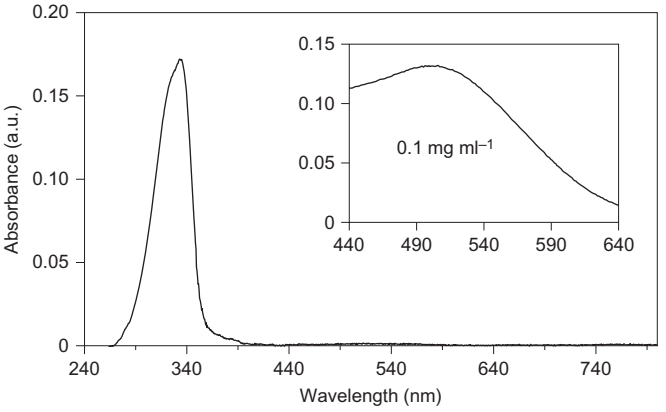

Figure 4 | Ultraviolet–visible absorbance data for [5]CPP. [5]CPP exhibits a major ultraviolet absorbance similar to that of other CPPs (1 μg ml^{-1}, $\lambda_{max} =$ 335 nm). Inset: As apparent by its red colour, a minor green absorbance from a HOMO–LUMO transition is also present (0.1 mg ml^{-1}, $\lambda_{max} =$ 502 nm). a.u., arbitrary units.

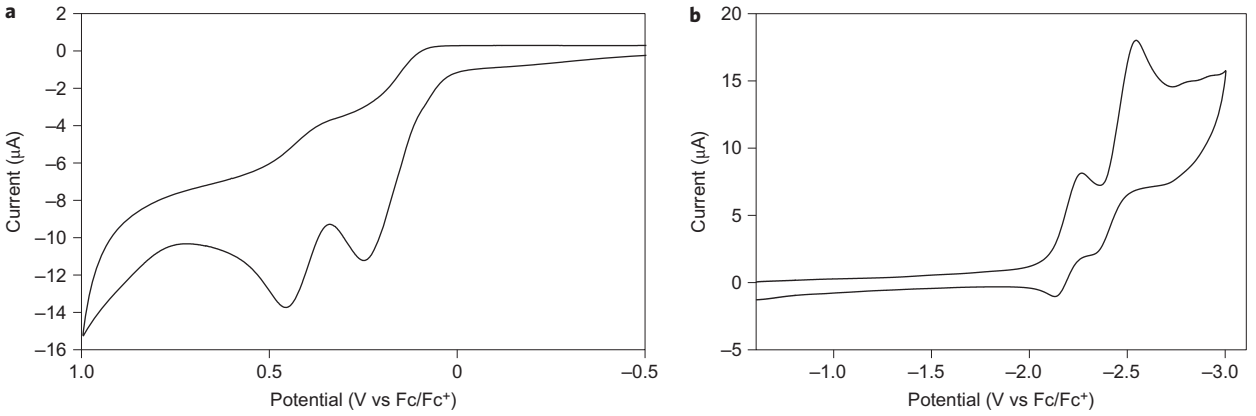

Figure 5 | Cyclic voltammetry of [5]CPP in THF. a,b, Two oxidation events (**a**) and two reduction events (**b**) were observed for **[5]CPP**. All these appeared to be pseudoreversible. **[5]CPP** has a lower oxidation potential and less-negative reduction potential than those of any CPP.

from a HOMO–LUMO transition that, forbidden in larger CPPs, starts to manifest in the smaller CPPs. As with **[6]CPP**, as a result of the weak oscillator strength of the HOMO–LUMO transition, there is no observable fluorescence in **[5]CPP**[49].

The oxidation and reduction potentials of **[5]CPP** were obtained by cyclic voltammetry, 1 mM in THF solution with 0.1 M n-Bu_4NPF_6 (Fig. 5). Interestingly, we observed two oxidation events with peak potentials of 0.25 and 0.46 V versus Fc/Fc^+ and two reductions with peak potentials of −2.27 and −2.55 V versus Fc/Fc^+. All four events appear to be pseudoreversible one-electron processes. **[5]CPP** has the lowest oxidation and least-negative reduction potential of any *para*-polyphenylene[22]. The narrow electrochemical gap combined with crystalline organization in the solid state make **[5]CPP** an excellent candidate as an organic semiconductor.

In conclusion, we report the synthesis of **[5]CPP**, the smallest carbon nanohoop. Our mild and high-yielding synthesis builds in a remarkable 119 kcal mol^{-1} strain energy in solution without heating. This work illustrates the success of rational chemical design applied to challenging carbon architectures and offers a room-temperature synthesis of a nonplanar aromatic hydrocarbon in the same class as corannulene[2], C_{60} fullerene[6] or grossly warped nanographene[50]. Studies of the inclusion of **[5]CPP** in devices and host–guest complexes will be reported in due course.

Note added in proof: The authors became aware of a further relevant paper that they would like to cite: Kayahara, E., Patel, V. K. & Yamago, S. Synthesis and Characterization of [5]Cycloparaphenylene *J. Am. Chem. Soc.* **136**, 2284–2287 (2014).

Methods

Preparation of macrocycle 2. To a 2 l flask equipped with a magnetic stir bar was added diboronic bispinacol ester **1** (3.74 g, 4.90 mmol, 1.00 equiv.) and THF (1,030 ml). The resulting solution was stirred until all the solid was in solution, at which point bis(triphenylphosphine)palladium(II) dichloride (0.346 g, 0.490 mmol, 0.100 equiv.) was added followed by H_2O (200 ml). To this yellow solution was added potassium fluoride (0.289 g, 4.90 mmol, 1 equiv.). The solution gradually turned bright orange over two hours and was allowed to stir open to air and at room temperature for an additional ten hours at which point palladium black had coated the inside of the flask. The crude reaction mixture was filtered through a pad of Celite to remove palladium. This filter cake was washed with dichloromethane (100 ml). The solution was extracted with dichloromethane (2 × 300 ml) and the resulting organic phase was washed with brine (500 ml). The organic phase was then dried over sodium sulfate and the solvent was removed at reduced pressure to give a yellow semisolid. This yellow semisolid was then washed with acetone (100 ml) to dissolve impurities and gave the product as a white solid, which was collected by vacuum filtration. This white solid (1.40 g, 52%) can be further purified on SiO_2 if necessary. The white solid was dissolved in minimal dichloromethane and loaded onto a short pad of silica. The product was eluted in 15% ethyl acetate in dichloromethane to give a pristine crystalline white solid (1.10 g, 44%); melting point (m.p.), 311–312 °C; ^{1}H NMR (400 MHz, $CDCl_3$), δ (ppm) 7.46 (d, J = 9.4 Hz, 4H), 7.43 (d, J = 9.4 Hz, 4H), 6.58 (d, J = 10.2 Hz, 2H), 6.00 (s, 4H), 5.73 (d, J = 10.2 Hz, 2H), 3.46 (s, 6H), 3.26 (s, 6H); ^{13}C NMR (100 MHz, $CDCl_3$), δ (ppm) 141.67, 141.29, 140.02, 133.91, 133.73, 128.90, 127.47, 125.09, 74.96, 73.68, 52.65, 51.27; infrared (neat), 3,026, 2,979, 2,936, 2,899, 2,820, 1,594, 1,497, 1,487, 1,464, 1,449, 1,398, 1,306, 1,275, 1,262, 1,221, 1,186, 1,170, 1,075, 1,017, 988, 955, 942, 887, 862, 845, 823, 758, 702, 670, 617, 577, 557, 514, 467 cm^{-1}; high-resolution mass spectroscopy (HRMS) (Q-TOF, ES+) *(m/z)*, $[M + Na]^+$ calculated for $C_{34}H_{32}O_4$ 527.2198, found 527.2205.

Preparation of reduced macrocycle 3. Macrocycle **2** (200 mg, 0.400 mmol, 1.00 equiv.) was dissolved in dry THF (150 ml) and cooled to −78 °C under N_2. Sodium naphthalenide (1 M; 2.00 ml, 2.00 mmol, 50.0 equiv.) was added dropwise to the stirring solution to give a deep-blue colour. This was allowed to stir for 40 minutes at which point methanol (1 ml) was added dropwise to give a clear yellow solution. The reaction was allowed to warm to room temperature at which point water (100 ml) and DCM (100 ml) were added. The aqueous layer was then extracted with DCM (2 × 100 ml). The combined organic layers were washed with water (3 × 100 ml), brine (1 × 100 ml) and dried over sodium sulfate before being filtered and concentrated down to a solid. The crude solid was adsorbed onto silica gel and washed with hexane (3 × 100 ml) to remove excess naphthalene. The product was eluted with a 1:1 mixture of ethyl acetate and DCM (200 ml). The solvent was then removed under vacuum to give the product as a white solid (160 mg, 91%); m.p., decomposition >350 °C; ^{1}H NMR (400 MHz, $CDCl_3$), δ (ppm) 7.42 (d, J = 8.6 Hz, 4H), 7.28 (d, J = 8.6 Hz, 4H), (dd, J = 10.4, 4.9 Hz, 4H), 6.05 (s, 4H), 5.63 (d, J = 10.4 Hz, 4H), 4.27 (t, J= 4.9 Hz, 2H), 3.21 (s, 6H); ^{13}C NMR (125 MHz, $CDCl_3$), δ (ppm) 143.04, 142.01, 138.19, 131.84, 131.60, 128.71, 127.31, 125.18, 74.85, 54.15, 36.39; infrared (neat), 3,052, 2,990, 2,930, 2,898, 2,873, 2,820, 1,722, 1,703, 1,665, 1,592, 1,512, 1,487, 1,467, 1,454, 1,397, 1,360, 1,265, 1,220, 1,188, 1,170, 1,068, 1,012, 986, 961, 920, 883, 863, 851, 834, 814, 803, 770, 734, 704, 592, 582, 541, 488, 390 cm^{-1}; HRMS (Q-TOF, ES+) *(m/z)*, $[M + Na]^+$ calculated for $C_{12}H_{10}ClO_2$, 467.1987, found 467.1196.

Preparation of [5]CPP. Diisopropylamine (5.00 ml, 36.0 mmol, 48.0 equiv.) was added to dry toluene (650 ml) in a flame-dried round-bottom flask under N_2. This solution was cooled to 0 °C at which point 2.3 M n-butyl lithium in hexanes (9.60 ml, 22.0 mmol, 30.0 equiv.) was added dropwise and stirred for 20 minutes at 0 °C. Reduced macrocycle **3** (330 mg, 0.740 mmol, 1.00 equiv.) was dissolved in dry toluene (50.0 ml) and was added dropwise to the stirring solution of LDA. The reaction was warmed to room temperature and allowed to stir for two hours, which resulted in a deep ruby red solution, at which point it was quenched with 200 ml water. The solution was extracted with toluene (3 × 100 ml). The resulting organic phase was pooled and washed with water (3 × 200 ml), brine (1 × 200 ml) and dried over sodium sulfate before concentration under vacuum. Chromatography of the crude red solid on silica gel in pure DCM gave a solid red band that was collected and concentrated to give **[5]CPP** as brilliant-red needles (195 mg, 69% yield); m.p., decomposition >400 °C; ^{1}H NMR (400 MHz, $CDCl_3$), δ (ppm) 7.85 (s, 20H); ^{13}C NMR (125 MHz, $CDCl_3$), δ (ppm) 131.96, 126.57; infrared (neat), 3,005, 2,956, 2,922, 2,853, 1,666, 1,602, 1,549, 1,508, 1,478, 1,459, 1,415, 1,375, 1,342, 1,299, 1,259, 1,236, 1,180, 1,171, 1,120, 1,079, 1,053, 1,026, 956, 930, 843, 817, 767, 688, 635, 552, 463, 448, 429 cm^{-1}; MALDI-TOF *(m/z)*, $[M]^+$ calculated for $C_{30}H_{20}$ 380.16, found 380.86.

Received 26 November 2013; accepted 7 February 2014; published online 9 March 2014

References

1. Eaton, P. E. & Cole, T. W. Cubane. *J. Am. Chem. Soc.* **86,** 3157–3158 (1964).
2. Lawton, R. G. & Barth, W. E. Synthesis of corannulene. *J. Am. Chem. Soc.* **93,** 1730–1745 (1971).

3. Dauben, W. G. & Cargill, R. L. Photochemical transformations, VIII: the isomerization of Δ2,5-bicyclo[2.2.1]heptadiene to quadricyclo[2.2.1.$0^{2,6}$-$0^{3,5}$] heptane (quadricyclene). *Tetrahedron* **15,** 197–201 (1961).
4. Kammermeier, S., Jones, P. G. & Herges, R. Ring-expanding metathesis of tetradehydro-anthracene—synthesis and structure of a tubelike, fully conjugated hydrocarbon. *Angew. Chem. Int. Ed. Engl.* **35,** 2669–2671 (1996).
5. Kane, V. V., Wolf, A. D. & Jones, M. [6]Paracyclophane. *J. Am. Chem. Soc.* **96,** 2643–2644 (1974).
6. Scott, L. T. *et al.* A rational chemical synthesis of C_{60}. *Science* **295,** 1500–1503 (2002).
7. Hopf, H. *Classics in Hydrocarbon Chemistry* (Wiley-VCH, 2000).
8. Scott, L. T. Conjugated belts and nanorings with radially oriented *p* orbitals. *Angew. Chem. Int. Ed.* **42,** 4133–4135 (2003).
9. Parekh, V. C. & Guha, P. C. Synthesis of *p,p*-diphenylene disulfide. *J. Indian Chem. Soc.* **11,** 95–100 (1934).
10. Yamago, S., Watanabe, Y. & Iwamoto, T. Synthesis of [8]cycloparaphenylene from a square-shaped tetranuclear platinum complex. *Angew. Chem. Int. Ed.* **49,** 757–759 (2010).
11. Omachi, H., Matsuura, S., Segawa, Y. & Itami, K. A modular and size-selective synthesis of [*n*]cycloparaphenylenes: a step toward the selective synthesis of [*n,n*] single-walled carbon nanotubes. *Angew. Chem. Int. Ed.* **49,** 10202–10205 (2010).
12. Jasti, R., Bhattacharjee, J., Neaton, J. B. & Bertozzi, C. R. Synthesis, characterization, and theory of [9]-, [12]-, and [18]cycloparaphenylene: carbon nanohoop structures. *J. Am. Chem. Soc.* **130,** 17646–17647 (2008).
13. Srinivasan, M., Sankararaman, S., Hopf, H. & Varghese, B. Synthesis of buta-1,3-diyne-bridged macrocycles with (*Z*)-1,4-diethynyl-1,4-dimethoxycyclohexa-2,5-diene as the building block. *Eur. J. Org. Chem.* **2003,** 660–665 (2003).
14. Xia, J. & Jasti, R. Synthesis, characterization, and crystal structure of [6]cycloparaphenylene. *Angew. Chem. Int. Ed.* **51,** 2474–2476 (2012).
15. Golder, M. R., Wong, B. M. & Jasti, R. Photophysical and theoretical investigations of the [8]cycloparaphenylene radical cation and its charge-resonance dimer. *Chem. Sci.* **4,** 4285–4291 (2013).
16. Zabula, A. V., Filatov, A. S., Xia, J., Jasti, R. & Petrukhina, M. A. Tightening of the nanobelt upon multielectron reduction. *Angew. Chem. Int. Ed.* **52,** 5033–5036 (2013).
17. Iwamoto, T., Watanabe, Y., Sadahiro, T., Haino, T. & Yamago, S. Size-selective encapsulation of C_{60} by [10]cycloparaphenylene: formation of the shortest fullerene-peapod. *Angew. Chem. Int. Ed.* **50,** 8342–8344 (2011).
18. Xia, J., Bacon, J. W. & Jasti, R. Gram-scale synthesis and crystal structures of [8]- and [10]CPP, and the solid-state structure of C_{60}@[10]CPP. *Chem. Sci.* **3,** 3018–3021 (2012).
19. Hirst, E. S. & Jasti, R. Bending benzene: syntheses of [*n*]cycloparaphenylenes. *J. Org. Chem.* **77,** 10473–10478 (2012).
20. Omachi, H., Nakayama, T., Takahashi, E., Segawa, Y. & Itami, K. Initiation of carbon nanotube growth by well-defined carbon nanorings. *Nature Chem.* **5,** 572–576 (2013).
21. Darzi, E. R., Sisto, T. J. & Jasti, R. Selective syntheses of [7]–[12]cycloparaphenylenes using orthogonal Suzuki–Miyaura cross-coupling reactions. *J. Org. Chem.* **77,** 6624–6628 (2012).
22. Iwamoto, T., Watanabe, Y., Sakamoto, Y., Suzuki, T. & Yamago, S. Selective and random syntheses of [*n*]cycloparaphenylenes (*n*=8–13) and size dependence of their electronic properties. *J. Am. Chem. Soc.* **133,** 8354–8361 (2011).
23. Sisto, T. J., Golder, M. R., Hirst, E. S. & Jasti, R. Selective synthesis of strained [7]cycloparaphenylene: an orange-emitting fluorophore. *J. Am. Chem. Soc.* **133,** 15800–15802 (2011).
24. Kayahara, E., Iwamoto, T., Suzuki, T. & Yamago, S. Selective synthesis of [6]-, [8]-, and [10]cycloparaphenylenes. *Chem. Lett.* **42,** 621–623 (2013).
25. Kayahara, E., Sakamoto, Y., Suzuki, T. & Yamago, S. Selective synthesis and crystal structure of [10]cycloparaphenylene. *Org. Lett.* **14,** 3284–3287 (2012).
26. Sibbel, F., Matsui, K., Segawa, Y., Studer, A. & Itami, K. Selective synthesis of [7]- and [8]cycloparaphenylenes. *Chem. Commun.* **50,** 954–956 (2013).
27. Segawa, Y. *et al.* [9]Cycloparaphenylene: nickel-mediated synthesis and crystal structure. *Chem. Lett.* **40,** 423–425 (2011).
28. Segawa, Y. *et al.* Concise synthesis and crystal structure of [12]cycloparaphenylene. *Angew. Chem. Int. Ed.* **50,** 3244–3248 (2011).
29. Ishii, Y. *et al.* Size-selective synthesis of [9]–[11] and [13]cycloparaphenylenes. *Chem. Sci.* **3,** 2340–2345 (2012).
30. Hitosugi, S., Nakanishi, W., Yamasaki, T. & Isobe, H. Bottom-up synthesis of finite models of helical (*n,m*)-single-wall carbon nanotubes. *Nature Commun.* **2,** 492 (2011).
31. Yagi, A., Segawa, Y. & Itami, K. Synthesis and properties of [9]cyclo-1,4-naphthylene: a π-extended carbon nanoring. *J. Am. Chem. Soc.* **134,** 2962–2965 (2012).
32. Matsui, K., Segawa, Y. & Itami, K. Synthesis and properties of cycloparaphenylene-2,5-pyridylidene: a nitrogen-containing carbon nanoring. *Org. Lett.* **14,** 1888–1891 (2012).
33. Sisto, T. J., Tian, X. & Jasti, R. Synthesis of tetraphenyl-substituted [12]cycloparaphenylene: toward a rationally designed ultrashort carbon nanotube. *J. Org. Chem.* **77,** 5857–5860 (2012).
34. Wong, B. M. Optoelectronic properties of carbon nanorings: excitonic effects from time-dependent density functional theory. *J. Phys. Chem. C* **113,** 21921–21927 (2009).
35. Frisch, M. J. *et al. Gaussian 09, Revision D.01* (Gaussian Inc., 2009).
36. Nakamura, E., Tahara, K., Matsuo, Y. & Sawamura, M. Synthesis, structure, and aromaticity of a hoop-shaped cyclic benzenoid [10]cyclophenacene. *J. Am. Chem. Soc.* **125,** 2834–2835 (2003).
37. Anslyn, E. & Dougherty, D. *Modern Physical Organic Chemistry* 183–185 (University Science Books, 2008).
38. Punna, S., Díaz, D. D. & Finn, M. G. Palladium-catalyzed homocoupling of arylboronic acids and esters using fluoride in aqueous solvents. *Synlett* **2004,** 2351–2354 (2004).
39. Moreno-Mañas, M., Pérez, M. & Pleixats, R. Palladium-catalyzed Suzuki-type self-coupling of arylboronic acids. A mechanistic study. *J. Org. Chem.* **61,** 2346–2351 (1996).
40. Tobe, Y., Jimbo, M., Saiki, S., Kakiuchi, K. & Naemura, K. Unusual reactivity of [6]paracyclophane toward alkyllithiums. *J. Org. Chem.* **58,** 5883–5885 (1993).
41. Tobe, Y. *et al.* Synthesis and molecular structure of (*Z*)-[6]paracycloph-3-enes. *J. Am. Chem. Soc.* **109,** 1136–1144 (1987).
42. Jagadeesh, M. N., Makur, A. & Chandrasekhar, J. The interplay of angle strain and aromaticity: molecular and electronic structures of [0*n*]paracyclophanes. *J. Mol. Model.* **6,** 226–233 (2000).
43. Allinger, N. L., Walter, T. J. & Newton, M. G. Synthesis, structure, and properties of the [7]paracyclophane ring system. *J. Am. Chem. Soc.* **96,** 4588–4597 (1974).
44. Tobe, Y. *et al.* Synthesis, structure and reactivities of [6]paracyclophanes. *Tetrahedron* **42,** 1851–1858 (1986).
45. Baran, P. S. & Burns, N. Z. Total synthesis of (±)-haouamine A. *J. Am. Chem. Soc.* **128,** 3908–3909 (2006).
46. Takiguchi, H., Ohmori, K. & Suzuki, K. Synthesis and determination of the absolute configuration of cavicularin by a symmetrization/asymmetrization approach. *Angew. Chem. Int. Ed.* **52,** 10472–10476 (2013).
47. Nikolaev, A. V., Dennis, T. J. S., Prassides, K. & Soper, A. K. Molecular structure of the C_{70} fullerene. *Chem. Phys. Lett.* **223,** 143–148 (1994).
48. Scott, L. T. *et al.* A short, rigid, structurally pure carbon nanotube by stepwise chemical synthesis. *J. Am. Chem. Soc.* **134,** 107–110 (2011).
49. Fujitsuka, M., Cho, D. W., Iwamoto, T., Yamago, S. & Majima, T. Size-dependent fluorescence properties of [*n*]cycloparaphenylenes (*n*=8–13), hoop-shaped π-conjugated molecules. *Phys. Chem. Chem. Phys.* **14,** 14585–14588 (2012).
50. Kawasumi, K., Zhang, Q., Segawa, Y., Scott, L. T. & Itami, K. A grossly warped nanographene and the consequences of multiple odd-membered-ring defects. *Nature Chem.* **5,** 739–744 (2013).

Acknowledgements

This work was supported by a National Science Foundation CAREER award (CHE-1255219), an Alfred P. Sloan Research Fellowship and a Boston University Ignition Award. The authors gratefully acknowledge J. Bacon (Boston University) for crystal-structure determination.

Author contributions

E.R.D. and P.J.E. conceived the project, designed and carried out the experiments, performed the calculations, analysed the data and wrote the manuscript with equal contribution. As such, E.R.D. and P.J.E. are credited as co-first authors. R.J. played a critical role in discussion of the experimental design, project direction, experiments and results, and preparation of the manuscript.

Additional information

Supplementary information and chemical compound information are available in the online version of the paper. Reprints and permissions information is available online at www.nature.com/reprints. Correspondence and requests for materials should be addressed to R.J.

Competing financial interests

The authors declare no competing financial interests.